Nanostructured ZnO thin film with improved optical and electrochemical properties prepared by hydrothermal electrochemical deposition technique

Indranil Biswas, Mousumi Majumder, Piyali Roy (Kundu), Debadrita Mukherjee, Ashim Kumar Chakraborty ✉

Material Characterization and Instrumentation Division, CSIR-Central Glass and Ceramic Research Institute, Jadavpur, Kolkata – 700032, India
✉ *E-mail: ashim3121@gmail.com*

Published in Micro & Nano Letters; Received on 11th December 2015; Revised on 5th April 2016; Accepted on 11th April 2016

Zinc oxide (ZnO) thin films were grown on fluorine-doped tin oxide coated glass substrate by the hydrothermal electrochemical deposition (HTED) route using slightly acidic aqueous zinc acetate solution at 80°C and were characterised by various techniques. The deposited films showed n-type behaviour with improved carrier concentration. The steady state photocurrent densities were found to be 0.4 mA/cm^2 (under UV irradiation) and 8 μA/cm^2 (under visible light illumination) at zero bias potential. Significant improvement of optical, electrochemical and photoelectrochemical properties of deposited films could be achieved using HTED technique.

1. Introduction: In the recent time, nanostructured zinc oxide (ZnO) has gained much interest for its direct wide band gap (3.2–3.37 eV) at room temperature. There are various applications of ZnO such as solar cells [1], high-performance nanosensors [2], display devices [3], optoelectronic devices [4], field-effect transistors and transparent electrodes etc. ZnO thin films can be synthesised using various techniques such as electrochemical deposition, pulsed laser deposition, sol–gel method, sputtering, chemical vapour deposition and spray pyrolysis. Electrochemical deposition technique is preferred due to its simplicity, economy and better control of the surface morphology and growth by manipulation of the deposition parameters [5]. Photo electrochemical (PEC) cells are currently being used in the conversion of solar energy to storable chemical energy. Non-toxicity, high electrochemical and thermal stability and direct optical band gap energy are a few characteristics of nanostructured ZnO that have made it an attractive material for PEC water splitting [6]. However, a very small percentage of light (mainly UV) in the solar spectrum can be absorbed by ZnO due to its wide optical band gap. Hence, various methods of synthesis of ZnO thin films with improved solar energy absorbing property is under investigation by several researchers. In this Letter, we report the synthesis of nanostructured ZnO thin films by a novel hydrothermal electrochemical deposition (HTED) method [7], characterisation of their structural, optical and electrochemical properties and also their application in PEC splitting of water. Simultaneous application of temperature, vapour pressure and electric field in the case of HTED is expected to be responsible for the change in morphological, optical and electrochemical parameters of the deposited ZnO thin films.

2. Experimental

2.1. Thin film deposition: HTED of ZnO on fluorine-doped tin oxide (FTO)-coated glass was carried out using Metrohm, Autolab AUt 85930 electrochemical workstation inside a HTED chamber (Fig. 1) in an aqueous solution of zinc acetate (50 mM) and potassium nitrate (0.1 M). The pH of the electrolyte was adjusted to ~5.8 using nitric acid (2 mM). Analytical grade chemicals (Merck) were used in this study. FTO-coated glass (Techinstro) of sheet resistance 10 Ω/sq was used as the working electrode (WE), and 99.99% pure zinc plate (Alfa Aesar) was used as the counter electrode (CE). The deposition was carried out in the potentiostatic mode with $V_{WE/CE} = -1.1$ V for a duration of 5 min. The deposition potential was obtained by cyclic voltammetry tests performed in the same electrochemical bath (Fig. 2). Zn^{+2} ions present in the electrolyte react with the hydroxide ions formed by electrochemical reduction. Thus, the deposition of ZnO on FTO-coated glass substrate can be explained by the following reactions.

$$NO_3^- + H_2O + 2e^- \rightarrow NO_2^- + 2OH^- \quad (1)$$

$$2H_2O + 2e^- \rightarrow H_2 + 2OH^- \quad (2)$$

$$CH_3COO^- + H_2O \rightarrow CH_3COOH + OH^- \quad (3)$$

$$Zn^{2+} + 2OH^- \rightarrow Zn(OH)_2 \rightarrow ZnO + H_2O \quad (4)$$

Uniform and well adhered ZnO thin films were deposited on FTO-coated glass substrate. The as deposited films were subjected to washing with distilled water, room temperature air drying for 24 hours and sintering at 400°C for one hour in air atmosphere with a temperature ramping rate of 5°C/min before characterisation.

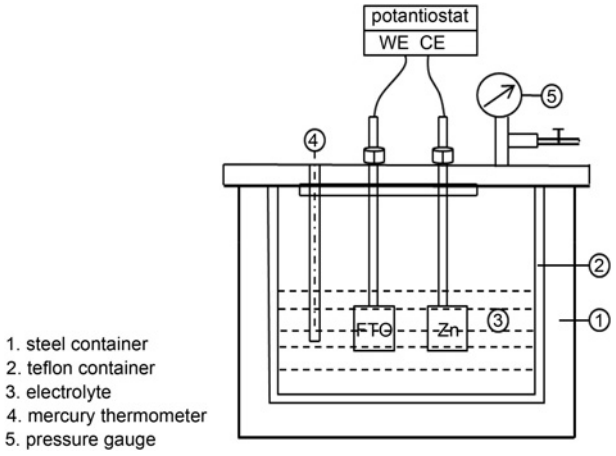

Fig. 1 *Schematic of in-house fabricated HTED chamber*

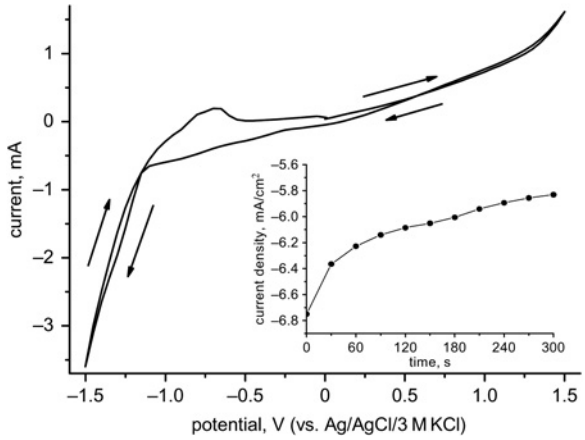

Fig. 2 *Cyclic voltammetry plot of FTO-coated glass electrode in zinc acetate (50 mM)and potassium nitrate (0.1 M) solution (pH = 5.8), (Inset) chronoamperometric curve*

2.2. Thin film characterisation: The X-ray diffraction data was collected using Bruker D8 Advance Davinci XRD System with Cu Kα radiation ($\lambda = 1.54$ A^0, 1.6 kW, 40 mA) used for phase identification of the deposited films. The surface morphology of the sample was determined using ZEISS (SIGMA) field emission scanning electron microscope (FESEM). X-ray photoelectron spectroscopy (XPS) measurements were performed using PHI 5000 Versa Probe II and the photoluminescence (PL) spectrum was measured by Perkin Elmer LS55 spectrophotometer at room temperature using an excitation wavelength of 350 nm. The optical absorption spectrum was captured using Shimadzu UV3600PC UV-Vis-NIR spectrophotometer was used to capture the optical absorption spectrum while the FTIR spectrum was recorded on a Perkin Elmer FTIR spectrometer using KBr technique in the range of 400 to 4000 cm^{-1}. PEC study was performed using a 24 W, $\lambda = 364$ nm, UV light (Philips), and a 100 W tungsten/halogen lamp (Philips), with a 420 nm glass filter (used to block UV light), a light choppers unit and Metrohm, Autolab AUt 85930 electrochemical workstation. The measurement was performed in a three-electrode cell with ZnO as the WE, Ag/AgCl/3 M KCl as the reference electrode and platinum – wire as the CE. 0.1 M aqueous solution of K_2SO_4 was used as the electrolyte. Capacitance-voltage (C-V) measurement in the dark was performed in the same three-electrode cell at a frequency of 1 kHz. An aqueous solution of 0.1 M KOH was used as the electrolyte.

3. Results and discussion

3.1. Structure, morphology and chemical state analysis: From X-ray diffraction study, all peaks identified correspond ZnO and no additional peaks corresponding to metallic zinc, or other oxides or hydroxides are present. The polycrystalline nature of the films is observed from the presence of multiple peaks of the ZnO phase (Fig. 3).

The average crystallite size (D_{hkl}) was calculated using Scherrer's (5) [8]

$$D_{hkl} = \frac{k\lambda}{\beta_{hkl}\cos\theta} \tag{5}$$

where k is Scherrer's constant ($k = 0.94$), λ is the wavelength of Cu Kα radiation (1.54 A^0), 2θ is the Bragg's diffraction angle, and β_{hkl} is the full width at the half maximum intensity of the characteristic peaks. From Scherrer's equation, the average crystallite size was found to be 13 nm. A strong peak along (002) plane indicates that the film is c-axis oriented. From the XRD pattern, hexagonal

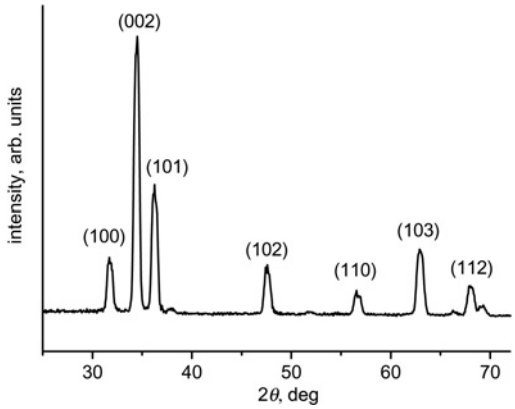

Fig. 3 *XRD patterns of the deposited ZnO thin film*

(wurtzite) structure of the thin film is confirmed. The unit cell parameters are calculated as $a = 3.255$ A^0, $c = 5.20616$ A^0 using the lattice equation of the wurtzite structure (6) [9]

$$a = d_{hkl}\sqrt{\frac{4}{3}\left(h^2 + hk + k^2\right) + l^2\left(\frac{a}{c}\right)^2} \tag{6}$$

where h, k and l are the Miller Indices and d_{hkl} is the interplanar distance. The calculated values of a and c are in good agreement with reported standard values (ICDD, pdf card no: 04-006-7189).

The FESEM micrograph shows a compact hexagonal wurtzite surface morphology with dense and uniform hexagonal grains along the c-axis. From the cross-sectional view of the FESEM micrograph, thickness of the film was measured to be 4.532 μm. It may be noted that there is a considerable difference in the crystallite size of the ZnO thin film as deduced from Scherrer's equation and from the FESEM micrograph. The larger size indicated in the FESEM images is probably due to the formation of grain agglomerates, as also experienced by previous researchers [10].

The chemical bonding state was investigated by using XPS. Fig. 5*a* shows the binding energy levels of Zn2p$_{3/2}$ (1021.3 eV) and Zn2p$_{1/2}$ (1044.3 eV), which confirms the presence of ZnO phase. The dominant peak at 530 eV in Fig. 5*b* is due to the electronic state of O1 s, which is consistent with the literature data of ZnO [11, 12]. The shoulder observed at a higher energy than the Zn-O bond state is probably due to the O-H bond state [13]. The O-H bond states are expected to exist on the surface, not in bulk, as no change was observed in the XPS spectra after a long time of air exposure.

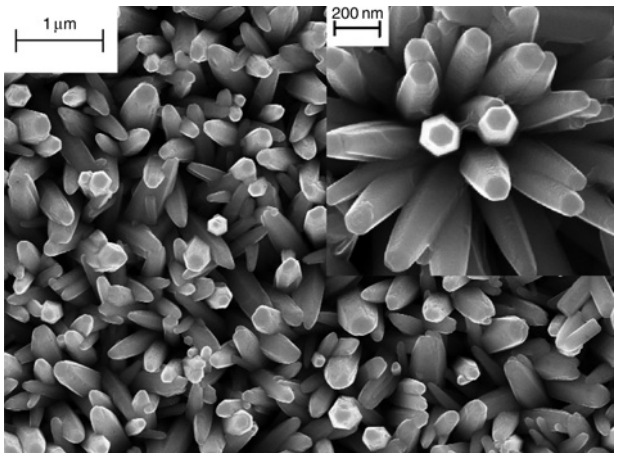

Fig. 4 *FESEM micrograph of the deposited ZnO thin film*

doi: 10.1049/mnl.2015.0528

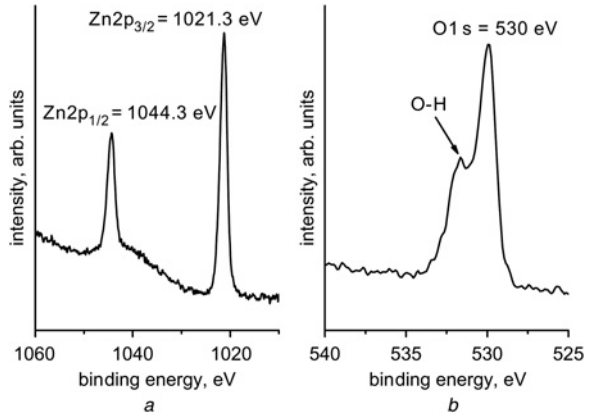

Fig. 5 *XPS spectra of the deposited ZnO thin film*
a $Zn2p_{3/2}$ and $Zn2p_{1/2}$ of ZnO
b O1 s of ZnO

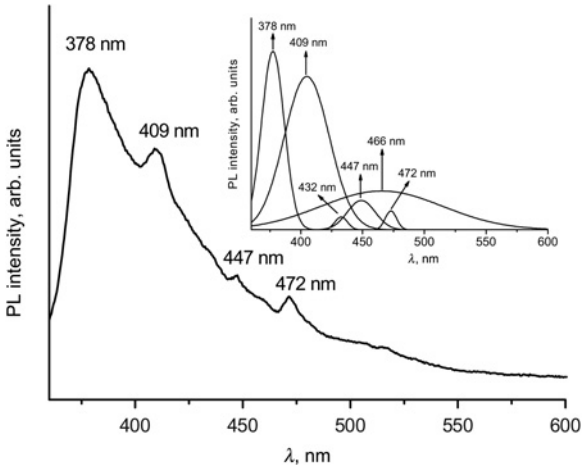

Fig. 7 *Room temperature PL spectra of the deposited ZnO thin film, (Inset) fitted peaks*

3.2. Optical properties: From the optical absorption spectra (Fig. 6) of the films it is observed that the films are good and moderate absorbers of UV and visible light, respectively. The visible light absorption may arise due to the intrinsic defects in the ZnO films like zinc vacancies, oxygen interstitials, and zinc interstitials [14]. The optical band gap was derived from the equation

$$(\alpha h\upsilon)^n = A\left(h\upsilon - E_g\right) \tag{7}$$

where $h\upsilon$ represents the photon energy, E_g is the optical band gap, A is a constant, α is the absorption coefficient, and n depends on the nature of the band gap ($n = 2$ for direct allowed transition). The intercept of the $(\alpha h\upsilon)^2 - h\upsilon$ plot with the $h\upsilon$ axis determines the band gap of the semiconductor. The band gap value for the deposited films was found to be 3.192 eV, which is lower than the theoretical band gap value (3.37 eV) of ZnO. The shift of the band gap may be attributed to the oxygen content on the surface of the film, as band gap values of O-rich ZnO films are smaller compared to Zn-rich films [15].

Fig. 7 shows the room temperature PL spectrum of the ZnO thin film deposited at 80°C at an excitation wavelength of 350 nm. It is observed that the spectrum consists of near-band edge as well as deep level emissions. Zhan *et al.* [16] have also reported both emissions, although from different defect centres, which are probably dictated by the processing conditions. Willander *et al.* [17] have reviewed the various intrinsic and extrinsic defects encountered in ZnO nanostructures, with their probable effect on the luminescence properties of the films.

A strong peak at 378 nm (~3.28 eV) near the band edge is attributed to the recombination of excitons [18]. The peak at 409 nm (~3.03 eV) may be due to electron transitions between the levels of zinc interstitials and valence band [19]. The small hump at 432 nm(~2.87 eV) may arise from the oxygen interstitials present in the film [20]. Emission appears at 447 nm (~2.77 eV) may be related to surface defects or ionised zinc vacancies [21]. The peak at 466 nm(~2.66 eV) may be ascribed to the transitions from the conduction band to the zinc vacancies [22]. The emission of 472 nm (~2.62 eV) is due to electron transitions between the levels of zinc interstitials and zinc vacancies [23].

In Fig. 8, FTIR spectrum shows a broad peak at 3400 cm^{-1} in the higher energy region which is due to O-H stretching. The main absorption peak at 555 cm^{-1} in the low region is due to Zn-O stretching of ZnO [24]. The IR absorption in the intermediate region is due to the vibration of ion impurities.

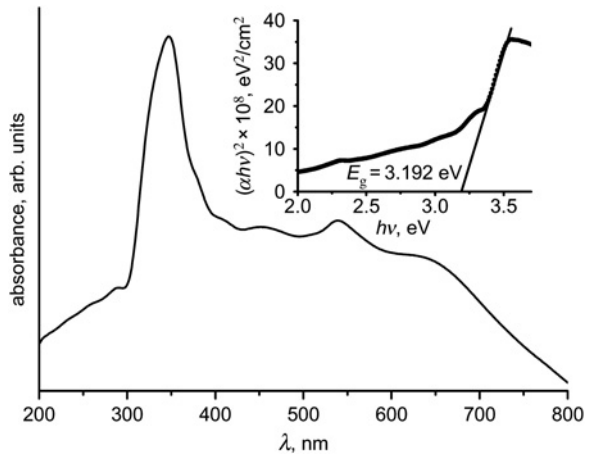

Fig. 6 *UV-Vis absorption spectra of the deposited ZnO thin film, (Inset) graphical determination of the optical band gap energy of the deposited ZnO thin film*

3.3. Photoelectrochemical and electrochemical properties: Electrochemical impedance spectroscopy (EIS) was carried out in dark, under UV ($\lambda = 364$ nm, Intensity = 6 mW/cm^2) irradiation and under visible light ($\lambda > 420$ nm, intensity = 100 mW/cm^2) illumination in 0.1 M K_2SO_4 solution at zero bias potential vs. Ag/AgCl/3 M KCl. The diameters of the semicircles in the Nyquist plot (Fig. 9) are equal to the charge transfer resistances. As seen, the charge transfer resistance of the deposited ZnO is

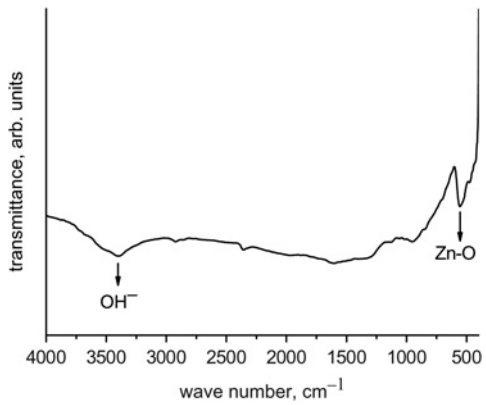

Fig. 8 *FT-IR spectrum of the deposited ZnO thin film*

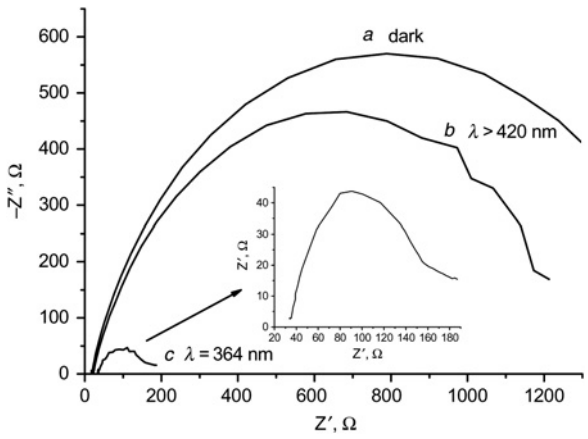

Fig. 9 *Nyquist plots of the deposited ZnO thin film*
a In dark
b Under visible illumination
c Under UV irradiation

much smaller under UV light irradiation than visible illumination and in dark. Such result indicates a dramatic enhancement of the interfacial charge transport and separation efficiency of photo generated charges under UV light irradiation.

Moreover, there is an acceptable enhancement of interfacial charge transport and separation efficiency of photo generated charges under visible light illumination ($\lambda > 420$ nm) than dark. This may be the reason for the enhanced PEC performance of the deposited ZnO thin film in the visible region.

The photocurrent density against time curve of ZnO films in 0.1 M K_2SO_4 solution was recorded at zero bias potential vs. Ag/AgCl/3 M KCl. The variation of observed photocurrent density with time is shown in Fig. 10. The steady state photocurrent density was 0.4 mA/cm^2 (under UV irradiation). Ivanauskas *et al.* [25] have reported photocurrent of ZnO thin films under UV irradiation ($\lambda = 366$ nm) as 200 μA/cm^2 at 0.6 V bias potential. In the present study, under illumination of visible light ($\lambda > 420$ nm), the

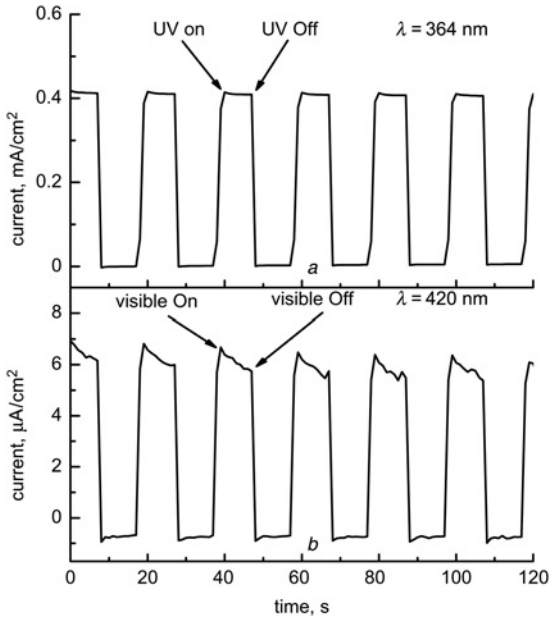

Fig. 10 *Photocurrent density against time curve of the deposited ZnO thin film in 0.1 M K_2SO_4 solution*
a Under UV irradiation
b Under visible light illumination

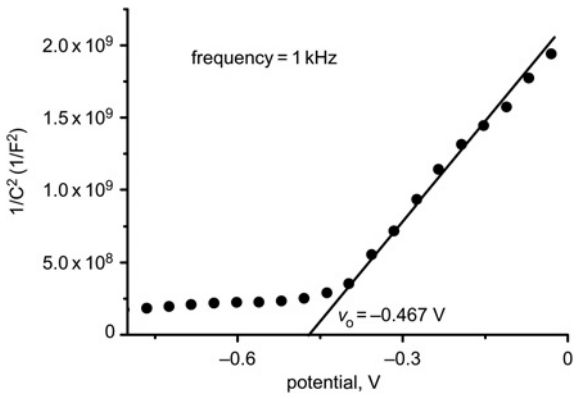

Fig. 11 *Mott–Schottky plot of the deposited ZnO thin film*

deposited ZnO thin films showed a photocurrent density of about 8 μA/cm^2, which is higher than the reported value of 1.7 μA/cm^2 [26] under identical illumination conditions. This considerable rise in photocurrent density can be explained by the electrochemical splitting of water, as there are no other redox entities present in the electrolyte. The higher vapour pressure during deposition of the film might have contributed to its surface O-H bonds and consequently lower bandgap energy, which allows more photon absorption and electron-hole pair generation [7]. Besides, the film has a uniform, well oriented, long nanorod structure, which might have enabled faster electron transport and enhanced diffusion lengths [27, 28]. Thus, the film deposition conditions, morphology and defect states were primarily responsible for the increase in current density of the ZnO film in UV and visible light conditions.

C-V data was analysed using Mott–Schottky equation (n-type) as

$$\frac{1}{C^2} = \frac{2}{e\varepsilon\varepsilon_o A^2 N}\left(V - V_{\text{fb}} - \frac{KT}{e}\right) \tag{8}$$

$$N = \frac{2}{e\varepsilon\varepsilon_o A^2 N} \tag{9}$$

$$V_{\text{fb}} = V_o - \frac{KT}{e} \tag{10}$$

where, V_{fb} is the flat-band potential, A is the electrode area, K is the Boltzmann constant, and T is the absolute temperature, ε_o is the permittivity of free space, e is the electronic charge, ε is the dielectric constant of ZnO, N is the carrier concentration and C is the capacitance between the ZnO layer and the electrolyte.

The positive slope of the curve in Fig. 11 confirms the n-type semiconductor behaviour of the deposited thin film. The calculated value of the flat-band potential is −0.492 V (vs. Ag/AgCl/3 M KCl). Carrier concentration is 8.9188×10^{20}/cm^3, which is consistent with the characteristic value of wurtzite structure of ZnO [29]. Due to high carrier concentration, a large number of electrons and holes are available for water splitting, which explains the enhanced PEC performance of the deposited ZnO thin films.

4. Conclusion: High quality ZnO films with band gap energy 3.192 eV could be deposited at 80°C using HTED. The typical hexagonal (wurtzite) structure of the thin films is confirmed by the XRD and FESEM studies. The EIS study, photocurrent measurement and Mott–Schottky plot of the deposited ZnO thin films show improved photoelectrochemical characteristics. Although the PEC performance under visible light illumination is comparatively low, the present work suggests that HTED could be a useful and economical process for preparing semiconducting ZnO electrode for PEC water splitting.

doi: 10.1049/mnl.2015.0528

5. Acknowledgment: The work has been carried out under the project ESC0103. Authors are grateful for the support of Director, CSIR-CG&CRI in carrying out this work. The help of AMMCD in recording the XRD spectrum and FESEM photographs is acknowledged. The authors are also grateful to the members of Sol–gel Division and NSMD for providing support in optical measurements.

6 References

[1] Wei Y.G., Xu C., Xu S., *ET AL.*: 'Planar waveguide-nanowire integrated three-dimensional dye-sensitized solar cells', *Nano Lett.*, 2010, **10**, pp. 2092–2096

[2] Yeh P.H., Li Z., Wang Z.L.: 'Schottky-gated probe-free ZnO nanowire biosensor', *Adv. Mater.*, 2009, **21**, pp. 4975–4978

[3] Sagar P., Kumar M., Mehra R.M.: 'Electrical and optical properties of sol-gel derived ZnO: Al thin films', *Mater. Sci.-Poland*, 2005, **23**, pp. 685–696

[4] Lu J.G., Fujita S., Kawaharamura T., *ET AL.*: 'Roles of hydrogen and nitrogen in p-type doping of ZnO', *Chem. Phys. Lett.*, 2007, **441**, pp. 68–71

[5] Paunovic M., Schlesinger M.: 'Fundamentals of electrochemical deposition, seconded' (John Wiley & Sons Inc., New York, 1998)

[6] Sakthivel S., Neppolian B., Shankar M.V., *ET AL.*: 'Solar photocatalytic degradation of azo dye : comparison of photocatalytic efficiency of ZnO and TiO2', *Sol. Energy Mater. Sol. C*, 2003, **77**, pp. 65–82

[7] Majumder M., Biswas I., Pujaru S., *ET AL.*: 'Cuprous oxide thin grown by hydrothermal electrochemical deposition technique', *Thin Solid Films*, 2015, **589**, pp. 741–749

[8] Azaroff L.V.: 'Elements of X-ray crystallography' (McGraw Hill Book Co, New York, 1968)

[9] Singh P., Kumar A., Deepak, *ET AL.*: 'ZnO nanocrystalline powder synthesized by ultrasonic mist-chemical vapour deposition', *Opt. Mater.*, 2008, **30**, pp. 1316–1322

[10] Chauhan D., Satsangi V.R., Dass S., *ET AL.*: 'Preparation and characterization of nanostructured CuO thin films for photoelectrochemical spiliting of water', *Bull. Mater. Sci.*, 2006, **29**, pp. 709–716

[11] Chen Y., Ko H., Hong S., *ET AL.*: 'Plasma-assisted molecular beam epitaxy for ZnO based II–VI semiconductor oxides and their heterostructures', *J. Vac. Sci. Technol.*, 2000, **B 18**, pp. 1514–1522

[12] Moulder J.F., Wtickle W.F.: 'Handbook of X-ray photoelectron spectroscopy', ULVAC. PHI. Inc., 1995

[13] Coppa B.J., Davis R.F., Nemanich R.J.: 'Gold Schottky contacts on oxygen plasma-treated, n-type ZnO(0001¯)', *Appl. Phys. Lett.*, 2003, **82**, pp. 400–402

[14] Guo P., Jiang J., Shen S., *ET AL.*: 'ZnS/ZnO heterojunction as photoelectrode: Type II band alignment towards enhanced photoelectrochemical performance', *Int. J. Hydrog. Energy*, 2013, **38**, pp. 13097–13103

[15] Kathalingam A., Kim M.R., Chae Y.S., *ET AL.*: 'Studies on electrochemically deposited ZnO thin films', *J. Korean Phys. Soc.*, 2009, **55**, pp. 2476–2481

[16] Zhan P., Liu W.W.C., Hu Y., *ET AL.*: 'Oxygen vacancy-induced ferromagnetism in un-doped ZnO thin films', *J. Appl. Phys.*, 2012, **111**, pp. 033501-1,5

[17] Willander M., Nur O., Sadaf J.R., *ET AL.*: 'Luminescence from zinc oxide nano structures and polymers and their hybrid devices', *Materials*, 2010, **3**, pp. 2643–2667

[18] Vanheusden K., Warren W.L., Seager C.H., *ET AL.*: 'Mechanisms behind green photoluminescence in ZnO phosphor powders', *J. Appl. Phys.*, 1996, **79**, pp. 7983–7990

[19] Fan X.M., Lian J.S., Zhao L., *ET AL.*: 'Single violet luminescence emitted from ZnO films obtained by oxidation of Zn film on quartz glass', *Appl. Surf. Sci.*, 2005, **252**, pp. 420–424

[20] Lin B., Fu Z., Jia Y.: 'Green luminescence centers in un-doped ZnO film deposited on silicon substrate', *Appl. Phys. Lett.*, 2001, **79**, pp. 943–945

[21] Wang J.M., Gao L.: 'Synthesis of uniform rod like, multi-pod-like ZnO whiskers and their photoluminescence properties', *J. Cryst. Growth*, 2004, **262**, pp. 290–294

[22] Mondal O., Pal M.: 'Strong and unusual violet-blue emission in ring shaped ZnO nano crystals', *J. Mater. Chem.*, 2011, **21**, pp. 18354–18358

[23] Tatsumi T., Fujita M., Kawamoto N., *ET AL.*: 'Intrinsic defects in ZnO films grown by molecular beam epitaxy', *Jpn. J. Appl. Phys.*, 2004, **43**, pp. 2602–2606

[24] Wang H., Xie C., Zeng D.: 'Controlled growth of ZnO by adding H_2O', *J. Cryst. Growth*, 2005, **277**, pp. 372–377

[25] Ivanauskas A., Šulčiūtė A., Valatka E.: 'Photoelectrochemical activity of electrophoretically deposited zinc oxide coatings on stainless steel substrates', *CHEMIJA*, 2013, **24**, pp. 97–102

[26] Wang M., Ren F., Cai G., *ET AL.*: 'Activating ZnO nano rod photoanodes in visible light by Cu ion implantation', *Nano Res.*, 2014, **7**, pp. 353–364

[27] Benkstein K.D., Kopidakis N., van de Lagemaat J., *ET AL.*: 'Influence of the percolation network geometry on electron transport in dye-sensitized titanium dioxide solar cells', *J. Phys. Chem. B*, 2003, **107**, pp. 7759–7767

[28] Frank A.J., Kopidakis N., van de Lagemaat J.: 'Electrons in nanostructured TiO_2 solar cells: transport, recombination and photovoltaic properties', *J. Coord. Chem. Rev.*, 2004, **248**, pp. 1165–1179

[29] Ashrafi A., Jagdish C.: 'Review of zincblende ZnO: stability of metastable ZnO phases', *J. Appl. Phys*, 2007, **102**, pp. 071101-1-12